Proceedings of ISFOG 2025
5TH INTERNATIONAL SYMPOSIUM ON
FRONTIERS IN OFFSHORE GEOTECHNICS
Nantes, France | June 9-13 2025

ISBN 978-2-85782-758-0

Pin foundation resistance in coarse gravel seabed - Numerical modelling with DEM

A. K. El Haj, E. Nicolini*, I. Terribile
CATHIE Group, Nanterre, France

T. Deglaire
HydroQuest, Meylan, France

**emilio.nicolini@cathiegroup.com*

ABSTRACT: Tidal energy is receiving interest as a viable source of renewable energy from offshore and is now ready for the first commercial farm offshore in France. The need of a technical and cost-effective solution has guided the industry to develop a turbine that can be installed on a purely gravity-based foundation structure. Such foundation will be placed in contact with the seabed by 3 isolated so-called "pins", which shall be able to bear the significant horizontal loads applied to the structure with the minimum vertical load. The pins shall grant such resistance on the rocky seabed as well as on the intermittent coarse gravel layer lying above, to cope with the observed seabed features. This paper presents the Discrete Element Method (DEM) particle model that was developed to study the pin behaviour and its holding capacity into the gravel layer. Different combinations of vertical loads and penetrations were explored and the corresponding holding capacities were determined. Further vertical penetration induced by the horizontal loading was also calculated. The calibrated DEM model enabled the design of the pin to grant the necessary capacity without exceeding the maximum allowed penetration for the service of the turbine.

Keywords: Tidal energy; gravity based foundation; pins; Discrete Element Method (DEM); holding capacity.

1 INTRODUCTION

Underwater turbines are emerging as an effective renewable energy technology, harnessing the steady motion of ocean tides to generate electricity. They provide dependable energy production while striving to reduce ecological impact.

Within the French offshore energy development plan, a tidal pilot project is underway in the Raz Blanchard area. This initiative involves installing tidal turbines on tripod foundations, with base 'pins' laying on the seabed. These pins will supply vertical bearing capacity and function as anchors, ensuring sufficient horizontal resistance as well.

A geological and geophysical campaign conducted to supply data relevant to the tidal turbine farm site have revealed that the site conditions are mainly granite rock, with a layer of gravels/boulders that was found on some of the turbine's locations. The gravel at the plant site offshore was studied via camera inspections and the videos were interpreted to estimate the geometrical properties of the gravels.

This paper describes the numerical analysis of tidal turbine foundation on such coarse gravel seabed. The goal of the study was to obtain some elements of the pin foundation behavior and determine the penetration and holding resistance against tidal loading.

2 DISCRETE ELEMENT METHOD (DEM)

The pin and the seabed are modelled using Discrete Element Method (DEM) developed by Cundall in 1971. DEM treats the material as an assembly of discrete particles. It can accurately simulate the interactions and movements of individual particles, and efficiently model contact and friction between discrete elements. It is a well-suited approach for very large displacements and dynamic simulations involving large deformations, collisions, and high-strain-rate phenomena. This made it suitable for addressing the studied problem.

3 FOUNDATION GEOMETRY

The tidal turbine is borne by a three-arm support, with the arms arranged in a plan distribution of approximately 135°-135°-90°, as depicted in Figure 1. Each arm touches the ground at a specific point, referred to as a "pin," which ensures that all three arms rest on the ground in a statically determined equilibrium, while the arm itself is not in contact with the seabed.

The rotation of the support around any axis will be negligible, if compared to the other componentes of displacement, due to the constraints of the overall structure, allowing it to mainly move in vertical and horizontal directions. This approach enables modeling just a single pin with sufficient accuracy from the soil mechanics point of view, instead of incorporating the entire foundation with all three pins. The upper section of the pin, which connects and forms the arm above the pin's top plate, is thus not part of the model. The detail view in Figure 1 presents the digital model of a preliminary pin geometry. To reduce computational effort, a half-model was used in the simulations, leveraging symmetry.

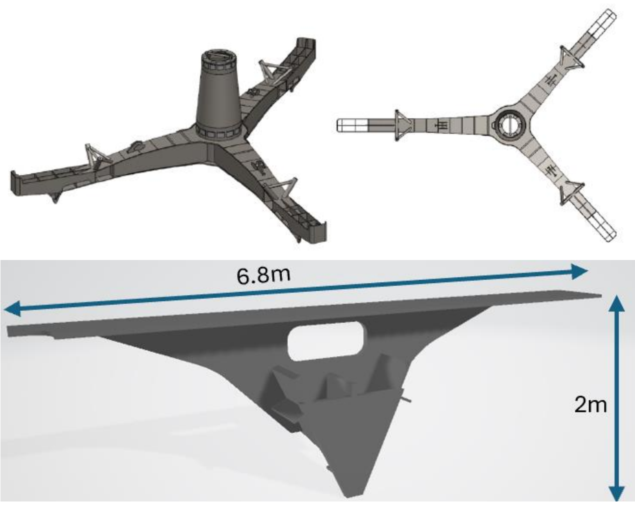

Figure 1. Geometry of the tidal turbine foundation and numerical model of the pin.

4 GRAVELS PROPERTIES

Based on the seabed video inspection survey, the shape of the gravels was observed to be rounded with no significant irregularities. The resulting particle size distribution based on the automatic interpretation of the obtained seabed images is presented in Figure 2, with a range of grain diameter from 2.5cm to 40cm.

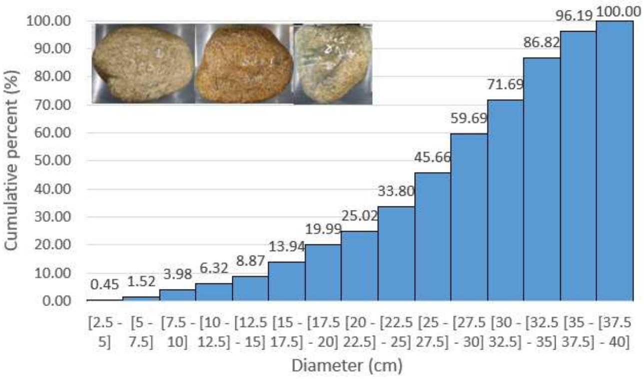

Figure 2. D2.5/40 PSD from site data

No geotechnical properties were available for the coarse gravel (the term gravel will be used in the paper for simplicity despite the grain size distribution is wider than that usually associated to gravel) layer. For this purpose, an angle of repose of around 37° was assumed for the gravels based on experience, and is confirmed if compared with the typical range of repose angles for granite material (35°-40°) from literature (Glover, 1997; materialtestingexpert.com). It is to be taken into account that the particles of the gravel at the site are rather rounded due to their origin (seabed rolling due to seabed current and tides), which was confirmed by the video inspections of the seabed. Values of the angle of repose in the range of 35°-40° are thus to be expected.

5 NUMERICAL MODEL

The Discrete element software PFC3D (Particle Flow Code) by Itasca (Itasca, 2021) was selected for the numerical simulation of the pin foundation behaviour.

The gravel and cobbles layer was modelled with spherical blocks as the photos from site did not show irregular (non-rounded) shape, with the aim of reducing computational effort. Any shape irregularity was compensated using a relevant contact model between balls, namely the rolling resistance linear model.

5.1 Contact model between gravels

The rolling resistance linear model, shown schematically in Figure 3 (Itasca, 2021), was used to numerically reproduce the contact between the gravels.

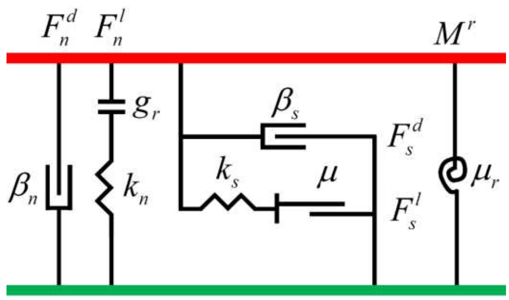

$$F_n^l \leftarrow M_l,\ \mathbf{F^d} \leftarrow M_d$$

Figure 3. Behaviour and rheological components of rolling resistance linear model.

The model consists of a linear-based model to which a rolling resistance mechanism is added. The effect of rolling resistance at contacts between particles, and associated energy dissipation, may be of major importance for many granular applications in both dense, quasistatic and dynamic regimes. In real granular systems, these mechanisms may have different micro-mechanical origins, such as adhesion of the contact area, or the effect due to surface roughness or non-sphericity about the contact point. This latter aspect is of great relevance to the present model, the gravel being modelled herein with spherical elements.

The main parameters of the rolling resistance linear model are listed as follows:

- the stiffness of the model is set to use an effective microscale elastic modulus of 100MPa and a normal-to-shear stiffness ratio of 2.5. These values correspond to settings usually used in DEM models to ensure the model is run in the rigid grain limit (GDR MiDi, 2004);
- the viscous damping normal critical ratio is set to a usual value of 0.2. Additionally, a local damping coefficient of 0.7 is used to help numerical convergence. Since the model is run in quasistatic conditions, it is not expected for these parameters to influence the results.
- the contact model friction coefficient μ and rolling friction μ_r coefficient parameters control the frictional and rolling-resistance strength of the contacts and the macroscopic internal friction angles of the gravels layer. These coefficients were calibrated to obtain a macroscopic angle of repose of about 37°.

5.2 Gravel properties calibration

The lifting cylinder test was simulated in PFC3D to check the particle parameters via the angle of repose of the gravel layer, as may be seen from Figure 4.

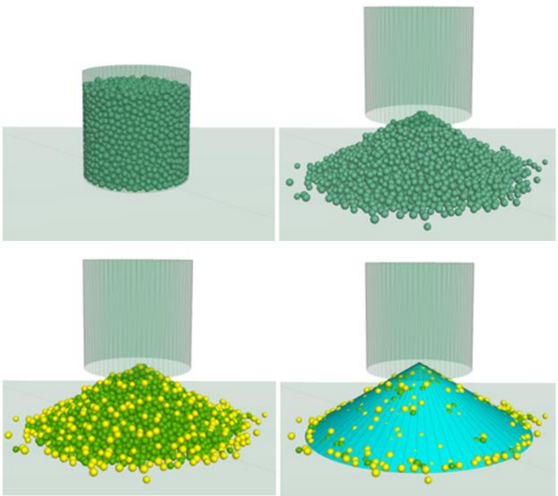

Figure 4 – Angle of repose simulation

It consists in forming a granular heap by lifting a cylindrical container initially filled with particles at rest under gravity. The chosen rolling resistance linear contact model was used, and the simulation was performed several times with varying values of the friction coefficient μ and rolling resistance coefficient μ_r to investigate their effect on the final shape of the heap. For each configuration, once the heap is formed after the cylinder is lifted, an algorithm is used to identify the balls situated at the extremity of the heap (yellow balls in Figure 4) and then fit a cone shape using the identified spheres. The angle of repose is finally computed as the angle of the fitted cone with respect to the horizontal plane.

5.3 Pin modelling procedure

Figure 5 below presents the pin-gravels interaction model developed in PFC3D.

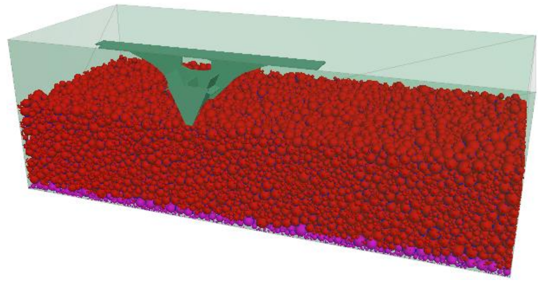

Figure 5 – PFC3D model of pin in gravels

The modelling steps of the pin in gravels may be described as follows:

- generate a cloud of overlapping balls of 15×6×3m, with a selected initial porosity (of 30% in this work), and respecting the particle size distribution obtained from site data (cf. Section 4). Contact between balls is governed by the rolling resistance linear model. Friction coefficients are set to their initial values at this stage to facilitate subsequent grain rearrangement, as a function of the target porosity level. Indeed, initial cloud porosity and initial friction coefficients mainly control the target porosity, together with the adopted granulometry. A local damping coef-ficient of 0.7 is imposed to the model to help numerical convergence in later steps;
- the model is cycled until the overlaps between the balls are eliminated. During this cycling process, the model is regularly calmed by setting all linear and rotational velocities to zero to prevent large velocities resulting from significant overlaps;
- gravity forces are applied to the model, and the model is solved and brought to the equilibrium state. The material is herein assumed to be fully drained, with water not modelled explicitly. The material's total mass density is considered, and a reduced gravity is used to account for the buoyancy. The grains are thus freely rearranged under gravity forces. The displacements are initialized to zero;
- after the balls being rearranged, the friction coefficient and the rolling friction coefficient are set to their final corresponding values;
- the balls at the bottom of the model are fixed in order to simulate base rugosity;

- the upper wall of the box is removed, and the pin geometry (.STL format) is imported such that the pin tip is at the level of the gravel layer surface. A friction coefficient of 0.5 is attributed to the interface between the steel and the balls;
- the pin vertical penetration is simulated using a controlled constant vertical velocity of 0.1m/s, which was selected after some sensitivity tests. Penetration is stopped when the entire height of the pin has penetrated the gravel layer. While penetrating, the resistance offered by the gravel to the pin penetration (R_v) is recorded, together with the vertical penetration (δ_v). Several model states are saved during pin penetration at equal intervals of 0.25m;
- from the above saved states, the pin is laterally displaced of at least 1m, by applying a lateral velocity to the pin while imposing a constant vertical force equal to R_v and constraining pin rotation. Several model states are saved at equal intervals of 0.2m.

6 RESULTS AND DISCUSSION

6.1 Granulometry reproduction

The granulometry observed on site was reproduced in PFC3D using the size distribution feature. To verify the accuracy of the result, a 2m dimension cubic box of spheres was created with a complete D2.5/40 granulometry as is shown in Figure 6. The cumulative volume percentage of the spheres in the created box was computed, and thus the numerical particle size distribution was determined. The PSD obtained from site data and that from generated spheres are superimposed in Figure 6, confirming that the granulometry was well reproduced.

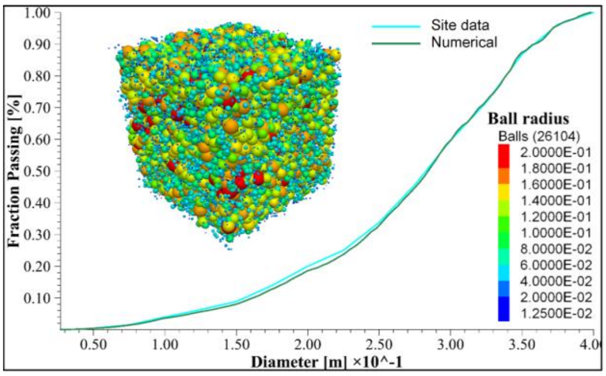

Figure 6 – Granulometry reproduction

6.2 Validation of the spherical particles model

In this section, the use of spherical balls along with the rolling resistance linear contact model is justified.

The vertical penetration of the pin foundation in the gravel layer was simulated for the case where a D20/40 distribution is considered with a target porosity of 44.7%. A comparison between two models, one with spherical balls and another with irregular rigid blocks, was performed in terms of accuracy and computation time. Within the two models, spherical and irregular blocks set-ups were generated both respecting the particle size distribution resulting from site data. For the irregular blocks model, 6 rigid block templates with various shapes were used as is shown in Figure 7. The penetration of the pin foundation within the two models is illustrated in the images in Figure 8.

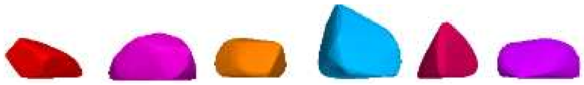

Figure 7 – Rigid block templates used in the model

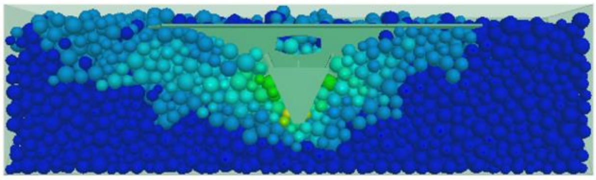

(a) Model with spherical balls

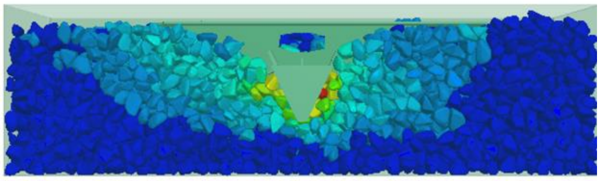

(b) Model with irregular blocks

Figure 8 – Models with (a) spherical balls and (b) irregular blocks

Results from performed simulations are presented in Figure 9 in terms vertical resistance versus vertical displacement curves. Results were shown to be comparable in terms of resistance, while a significant reduction in computation time was observed when using spherical blocks instead of irregular ones (8 minutes simulation for spherical blocks model instead of 120 minutes for irregular blocks model). The obtained results confirm the efficiency of using spherical blocks along with the rolling resistance linear model instead of irregular blocks.

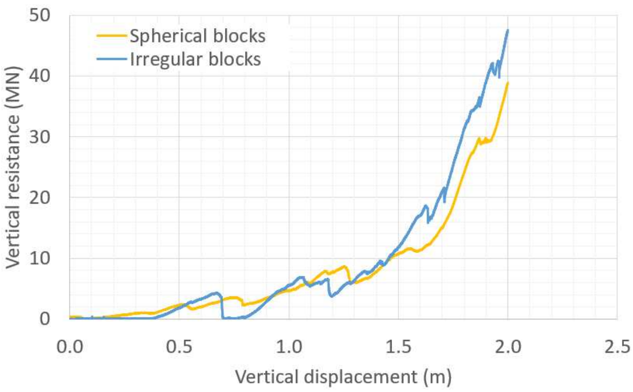

Figure 9 – Comparison between balls and blocks models

6.3 Model dimensions

A sensitivity analysis was conducted to optimize the model dimensions, ensuring that the boundaries are not too close to induce artificial effects, nor too far to excessively increase computational time. For this purpose, each analysis involved a simulation of vertical pin penetration to a depth of 1.5 meters, followed by a simulation of horizontal displacement of the pin over 1m while maintaining a constant vertical force equal to the corresponding vertical resistance.

Figure 10 presents the displacement field resulting from two models with different dimensions, where dark blue balls refers to zero displacement. It may be seen from the model on the left side of the figure that the displacement field touches the boundaries which may affect the accuracy of the results, indicating thus that the model dimensions were not sufficient. The model dimensions were progressively increased until the displacement field no longer touched the boundaries (despite 1m lateral displacement of the pin), as shown in the model on the right side of the figure, which was adopted for the rest of the analyses.

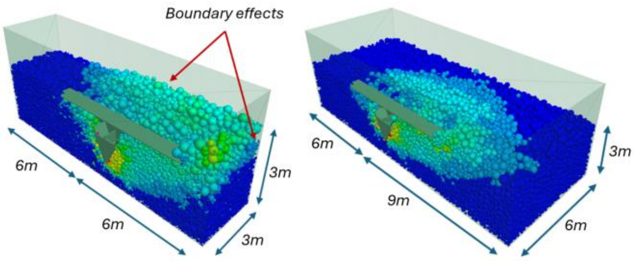

Figure 10 – Sensitivity analysis on model dimensions

6.4 Half model validation

Due to the symmetry in geometry and loading, a half model was proposed to reduce computational effort. To validate the accuracy of this reduced model, two vertical penetration simulations were conducted as illustrated in Figure 11 for the case of D10/40 distribution and a target porosity of 48.6%: one using a full model and the other using a half model that accounts for symmetry.

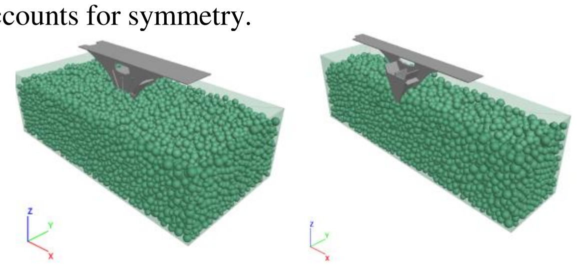

Figure 11 –Pin model: (left) full model (right) half model

Figure 12 presents the vertical resistance curves versus vertical displacement resulting from the two models. It was shown that the two curves were comparable, with a 30% reduction in the simulation time using the half model. The half model was therefore adopted for the study.

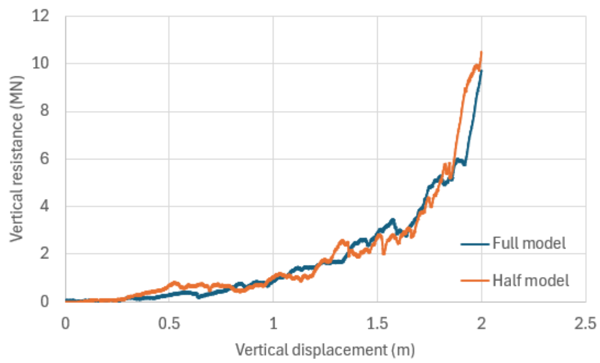

Figure 12 – Comparison between full model and half model results

6.5 Angle of repose simulation results

Figure 13 presents the results from the performed angle of repose simulations. Based on these results, a friction coefficient of 0.6, consistent with the value reported in (Potyondy, 2018) for friction between granite surfaces, and a rolling friction coefficient of 0.6 were selected such that a repose angle of about 37° is obtained.

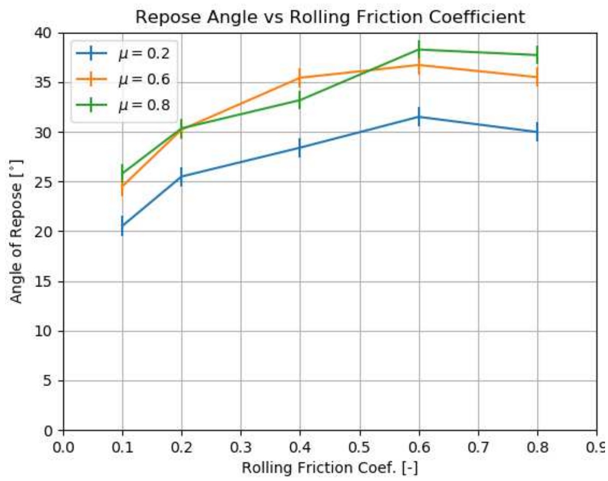

Figure 13 – Results of the angle of repose simulation

6.6 Pin simulation results

This section presents the results of the simulation of pin penetration in coarse gravel layer, followed by the application of horizontal loading at a certain pin penetration depth with the corresponding vertical force being constantly applied. The effect of layer porosity was also studied, by varying the adopted range of gravel size distribution (D10/40 and D2.5/40), then by controling relevant parameters intervening at the grain cloud generation and rearrangement stages, as discussed in section 5.3. Notice that the simulation time was shown to remarkably increase when smaller grain diameter is considered (i.e. larger distribution range) and a smaller porosity is used, which is related to the increase in the number of contacts in the model.

Figure 14 presents the vertical resistance of the pin versus the corresponding vertical displacement, for different cases of grain distribution range and layer porosity. The value of pin weight was indicated on the plot for reference. It can be observed from this figure that the vertical resistance exhibits an increase as the layer porosity decreases; however, the rate of this increase reduces as the porosity reaches lower values. This is also interpreted in Figure 15 in terms of pin penetration under its self-weight, where an exponential trend may be observed as a function of grain porosity.

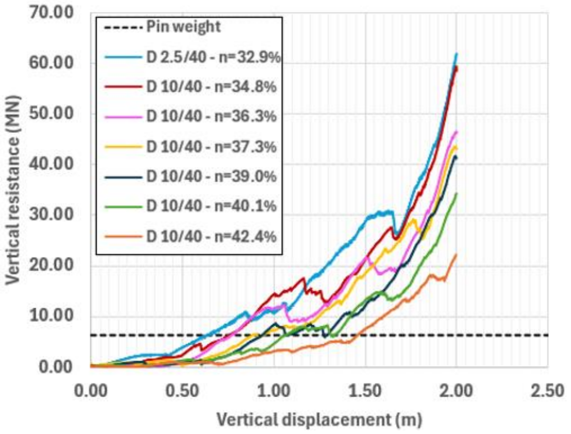

Figure 14 – Vertical resistance to pin penetration

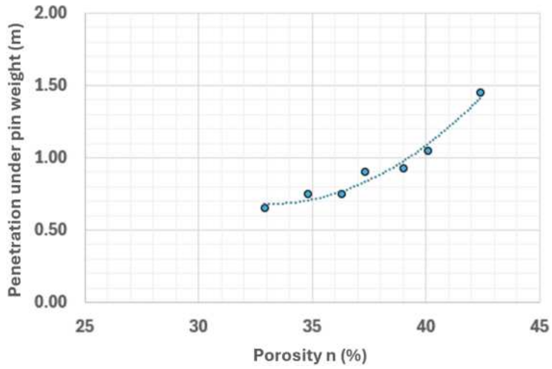

Figure 15 – Effect of porosity on pin penetration

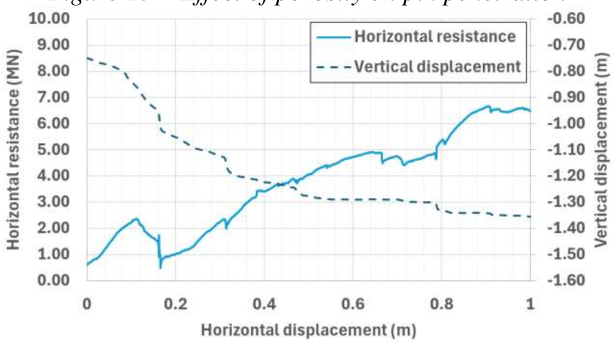

Figure 16 – Horizontal resistance and vertical penetration of the pin under horizontal loading

Figure 16 presents the horizontal resistance curve of the pin for the case D2.5/40 and n=32.9%,at a maintained constant vertical force corresponding to a vertical penetration of 0.75m. This figure also presents the vertical penetration of the pin induced by the horizontal loading. The pin penetration was shown to increase from 0.75m to nearly 1.36m.

7 CONCLUSIONS

This study analyzes the behavior of a pin foundation under vertical and horizontal loads in a coarse gravel seabed using DEM. The gravel granulometry was numerically reproduced and its representative model frictional parameters were calibrated, based on site visual inspection data and some relevant assumptions. The study offered insights into the foundation's holding capacity and the induced vertical penetration. The effect of grain size and layer porosity on the pin behaviour was highlighted within the study.

AUTHOR CONTRIBUTION STATEMENT

A.K. EL HAJ: Data curation, Formal Analysis, Writing- Original draft. **E. NICOLINI**: Methodology, Supervision and scientific lead, Conceptualization. **I. TERRIBILE**: Supervision, Writing- Reviewing and Editing. **T. DEGLAIRE**: Project administration, Writing- Reviewing and Editing.

ACKNOWLEDGEMENTS

We acknowledge that this study was conducted as part of a project assigned by HydroQuest to Cathie. We are grateful for the collaborative partnership and shared expertise, which have significantly contributed to the successful completion of this work.

REFERENCES

Cundall, P. A. and Strack, O. D. L. (1979). *A Discrete Numerical Model for Granular Assemblies. Géotechnique, 29*, pp.47-65.

G.D.R. Midi (2004). On dense granular flows. Eur. Phys. J. E 14, 341–365.

Glover, T.J. (1997). *Pocket Reference*. 2nd ed. Sequoia Publishing, Inc, 1997.

Itasca Consulting Group, Inc. (2021). *Particle Flow Code documentation*. Ver. 7.0. Minneapolis: Itasca.

Potyondy, D. (2018). A Flat-Jointed Bonded-Particle Model for Rock. 52nd U.S. Rock Mechanics/Geomechanics Symposium, Seattle, Washington, June 2018.

Material Testing Expert (2023). Angle of Repose, [online] Available at: https://www.materialtestingexpert.com/aggregate/angle-of-repose, accessed: 25/11/2024.